Journal of Advances in Modeling Earth Systems

RESEARCH ARTICLE
10.1029/2018MS001456

A Monolayer Partitioning Scheme for Droplets of Surfactant Solutions

J. Malila[1] and N. L. Prisle[1]

[1]Nano and Molecular Systems Research Unit, University of Oulu, Oulu, Finland

Key Points:
- We present a physically consistent model for predicting composition and thickness of a surface monolayer on aqueous solution droplets
- Model predictions are presented for binary and ternary water-surfactant-salt systems and compared to a Gibbsian model and experimental data
- The monolayer model predicts lower surface tensions than the Gibbsian model for droplet sizes relevant for atmospheric cloud activation

Supporting Information:
- Supporting Information S1

Correspondence to:
J. Malila and N. L. Prisle,
jussi.malila@oulu.fi;
nonne.prisle@oulu.fi

Citation:
Malila, J., & Prisle, N. L. (2018). A monolayer partitioning scheme for droplets of surfactant solutions. *Journal of Advances in Modeling Earth Systems*, *10*, 3233–3251. https://doi.org/10.1029/2018MS001456

Received 26 JUL 2018
Accepted 4 DEC 2018
Accepted article online 7 DEC 2018
Published online 25 DEC 2018

Abstract Bulk-surface partitioning of surface active species affects both cloud droplet activation by aerosol particles and heterogeneous atmospheric chemistry. Various approaches are given in the literature to capture this effect in atmospheric models. Here we present a simple, yet physically self-contained, monolayer model for prediction of both composition and thickness of the surface layer of an aqueous droplet. The monolayer surface model is based on assuming a finite surface layer and mass balance of all species within the droplet. Model predictions are presented for binary and ternary aqueous surfactant model systems and compared to both experimental and model data from the literature and predictions using a common Gibbsian model approach. Deviations from Gibbsian surface thermodynamics due to volume constraints imposed by the finite monolayer lead to stronger predicted surface tension reduction at smaller droplet sizes with the monolayer model. Process dynamics of the presented monolayer model are also contrasted to other recently proposed approaches to treating surface partitioning in droplets, with different underlying assumptions.

Plain Language Summary Aerosol particles in Earth's atmosphere are vital for the water cycle and climate. Many of these particles contain surface active organic material with an innate tendency to accumulate in water surfaces, including those of small cloud droplets. This may decrease surface tension and promote growth of a droplet within a cloud, but it is challenging to capture the effect directly in atmospheric simulations. Current models often rely on the time-tested Gibbsian thermodynamics, where the surface accumulation of molecules is calculated with respect to an idealized two-dimensional surface. Compared to experiments, this representation does not always capture the behavior of real solutions, especially in case of small droplets. In this work, we develop an alternative model, where the surface is treated as a thin layer with average thickness of a single molecule. This monolayer model gives physically reasonable results, which can be directly compared to both experimental measurements of surface properties, and assumptions used in climate and weather models. The monolayer model therefore provides a new tool to address one the largest uncertainties concerning Earth's energy balance and our understanding of climate change.

1. Introduction

Partitioning of surface active species (surfactants) to aqueous surfaces has significant effects on hygroscopic growth (Giddings & Baker, 1977; Hansen et al., 2015) and activation of atmospheric aerosol particles into clouds droplets (Ovadnevaite et al., 2017; Prisle et al., 2010; Ruehl et al., 2016), as well as on heterogeneous chemistry (Brüggemann et al., 2017; Öhrwall et al., 2015; Prisle, Ottosson, et al., 2012; Romakkaniemi et al., 2011; Rossignol et al., 2016; Schwier et al., 2011) at droplet surfaces, all processes that directly affect the radiative climate forcing due to aerosols. For concise reviews of various potential surfactant effects, we refer, for example, to McFiggans et al. (2006) and Donaldson and Vaida (2006). In general, it is computationally too expensive to incorporate an explicit treatment of surface partitioning directly into large-scale atmospheric models. Instead, simulations using various parameterizations based on different physical treatments—or thermodynamic frameworks—of surface partitioning suggest that surfactant effects contribute some of the largest uncertainties to predictions of cloud droplet number concentrations and effective radiative climate forcing due to aerosol-cloud interactions (Ghan et al., 2011; Prisle, Asmi, et al., 2012). According to Köhler (1936) theory, the critical saturation ratio S_c required for activation of a (soluble) particle into a cloud droplet is given by the maximum of

$$S = a_w \exp\left(\frac{2\sigma v_w}{kTR}\right), \quad (1)$$

where σ is the surface tension of the droplet with radius R, v_w the molecular volume of water in the droplet, and k and T denote the Boltzmann constant and temperature, respectively (McFiggans et al., 2006). In confined systems like activating cloud droplets, surface partitioning of various species within the solution can affect both the water activity (Raoult) term a_w and the exponential curvature (Kelvin) term (Prisle et al., 2008; Sorjamaa et al., 2004). The latter effect is directly modulated by the resulting droplet surface tension, which similarly to the droplet water activity is expressed as a function of the internal, or droplet bulk, composition. Whether the surfactant effects on both Raoult and Kelvin terms, or mainly on either the surface tension depression or water activity, are significant for cloud droplet formation in the atmosphere has been a recurrent research topic over the past 20 years.

Here we review existing approaches for the treatment of bulk-surface partitioning in aqueous droplets and present a new physically consistent partitioning scheme, based on a semiempirical relation between the surface tension and surface composition and on the conservation of mass within a solution droplet. We restrict our development to equilibrium surfaces, although it can be readily extended to nonequilibrium systems by incorporating dynamic surface tension (Kristensen et al., 2014; Nozière et al., 2014). We also do not here consider systems with nonequilibrium diffusion or solubility limitations (e.g., Pajunoja et al., 2015), which are not likely be important for hygroscopic systems outside the coldest and driest atmospheric conditions (Rothfuss et al., 2018). The presented framework may however be extended to include such processes as well. Finally, we focus the present description on the partitioning processes within the droplet, rather than their effects on cloud activation. Resulting effects on droplet activation thermodynamics will be the subject of detailed treatment in future work.

2. Background

Already more than 40 years ago, Hänel (1976) proposed a correction to the surface tension of cloud droplets, compared to pure water, due to the presence of surface active compounds in the droplets. Shulman et al. (1996) and Facchini et al. (1999) later recognized the potential importance of reduced droplet surface tension for the climatic impacts of clouds but did not consider the partitioning of surfactant molecules between the droplet bulk and surface. Both Bianco and Marmur (1992) and Laaksonen (1993) noted how the bulk-surface partitioning results in size-dependent surface tension of finite-sized droplets. This becomes important for cloud microphysics when measured surface tensions are reported and parameterized as functions of (macroscopic) bulk solution composition, whereas bulk-surface partitioning changes the droplet bulk (and surface) composition, and the resulting surface tension, for small droplets, even as the overall composition remains the same (Prisle et al., 2008; Sorjamaa et al., 2004).

Several approaches to describe bulk-surface partitioning have been used in atmospheric models; an overview is given in Table 1. Models are broadly classified according to their treatment of the surface as either a Gibbs' dividing surface, a monolayer or a multilayer, and on the equation-of-state (EoS, understood in a wide sense as a relation between surface tension and other variables of state) employed. Treatments beyond a thermodynamic description, such as molecular dynamic simulations (e.g., Chakraborty & Zachariah, 2011; Daskalakis et al., 2015; Li et al., 2010; Sun et al., 2013), are not considered here. Heterogeneous nucleation models including bulk-surface partitioning (Djikaev & Ruckenstein, 2014; Gorbunov et al., 1998) are also not included in Table 1, as the partitioning here is so deeply embedded in the overall thermodynamic description of the cluster that it cannot be separated out in a straightforward manner.

The Gibbsian two-dimensional models are based on combining a given EoS with the Gibbs (1878) adsorption equation (see also Adamson & Gast, 1997), which at constant temperature has the form

$$\mathrm{d}\sigma = -\sum_i \Gamma_i \mathrm{d}\mu_i. \quad (2)$$

Equation (2) gives the dependence of surface tension σ on chemical potentials μ_i and adsorptions Γ_i—in the form of surface excess numbers of molecules with respect to the area of the chosen dividing surface—of all droplet components i. The dividing surface is a two-dimensional mathematical concept separating two

Table 1
Bulk-Surface Partitioning Schemes Used in Atmospheric Models

Author(s)	EoS	Notes
Gibbsian 2-D surface		
Li et al. (1998); Abdul-Razzak and Ghan (2004)	S–L	Droplet equimolar with respect to water and salt
Sorjamaa et al. (2004); Sorjamaa and Laaksonen (2006)	S–L	No partitioning of salt with respect to water
Prisle et al. (2008, 2010)		
Topping (2010); Raatikainen and Laaksonen (2011)	S–L	Analytic approximations for numerical models
Monolayer		
Ellison et al. (1999)	LLPS	Full phase separation
Cai and Griffin (2005)	B–S–P	
Prisle et al. (2011)	LLPS	Full phase separation (can also be a multilayer) $\sigma = \sigma_w$
Prisle et al. (2011); Ruehl et al. (2016)	S–L	
Ruehl and Wilson (2014)	2DvdW	
Ruehl et al. (2016)	CF	
Ovadnevaite et al. (2017)	LLPS	Allows partial surface coverage, fixed surface thickness δ_{min}
Multilayer		
Pöschl et al. (2007)	KL	

Note. EoS = equation-of-state; SL = Szyszkowksi-Langmuir; LLPS = liquid-liquid phase separation; BSP = Butler-Sprow-Prausnitz; 2DvdW = 2-D van der Waals; CF = compressed film; KL = kinetic Langmuir.

phases, here the solution droplet and surrounding air. Therefore, Γ_i can assume both positive and negative values, with sign and magnitude depending on the definition (including position) of the dividing surface. Alternatively, the surface can be described in thermodynamic terms as a monolayer or multilayer (Defay et al., 1966; Rusanov, 1978). In such monolayer—and by extension, multilayer—models, the surface is considered as a finite layer of molecules with partial coverage $0 \leq \theta \leq 1$, and all adsorptions Γ_i are, by construction, positive.

Previously, there has been some conceptual confusion regarding the physical interpretation of surface quantities derived from two-dimensional versus finite surface (monolayer) models. To illustrate this, we consider the often used semiempirical von Szyszkowski (1908) surface tension model (see also Adamson & Gast, 1997)

$$\sigma = \sigma_w(T) - A \ln\left(1 + \frac{B}{C_{sft}}\right). \tag{3}$$

Here σ_w is the surface tension of the pure solvent—water (denoted "w"), in the case of atmospherically relevant cloud droplets—and C_{sft} is the volumetric molar or mass concentration of the surface active solute (denoted "sft"). For the macroscopic systems involved in experimental measurements of surface tension isotherms, C_{sft} refers to the observed surfactant concentration in the system, which has a negligible contribution from the surface. In finite-sized droplets, the surface contribution may become significant, and C_{sft} is thus interpreted as the concentration of surfactant specifically in the droplet bulk, for which the surface tension relation is well-defined from macroscopic measurements. Currently, there are no standard methods to provide such a relation directly from measurements on droplet sizes relevant for cloud activation. A and B in equation (3) are compound-specific parameters, which can be interpreted via equation (2) in terms of surface excess quantities (Adamson & Gast, 1997; Langmuir, 1917). Alternatively, as a limiting case of the monolayer model by Boyer et al. (2015) for strong surfactants with physically bounded quantities (i.e., a saturated monolayer, with maximum thickness of one monolayer, and nonnegative surface quantities), parameter A can specifically be interpreted as the normalized maximum adsorption Γ_{sft}^{∞} of the surfactant, that is, the density of closely packed surfactant molecules per unit surface area. In the Gibbsian approach, this interpretation also follows from equation (2) with a suitable definition of the dividing surface; however, this specific condition may simultaneously result in negative adsorptions Γ_i for other species in the solution, which

contradict the concept of physical surface layer. Extra care must therefore be taken when comparing parameters obtained from conceptually different surface frameworks, as well as when comparing model predictions to experimental results.

Gibbsian surface thermodynamics were first applied in cloud microphysics by Li et al. (1998) to predict bulk-surface partitioning for model systems mimicking the behavior atmospherically relevant surfactant solutions. Another formulation was provided by Sorjamaa et al. (2004) to more comprehensively include partitioning effects in both terms of the Köhler equation (1) and later revised by Prisle et al. (2010). Each of these, and related, approaches solve the adsorption equation (2) directly, whereas Topping (2010) and Raatikainen and Laaksonen (2011) each provide an analytic approximation for a such solution to facilitate computationally efficient implementation to larger-scale frameworks. The latter has, for example, been adopted by Petters and Kreidenweis (2013) and Petters and Petters (2016) to include surface partitioning into the κ-Köhler framework.

For a finite monolayer, equilibrium between bulk and surface can be given in terms of the Butler-Sprow-Prausnitz equation (Butler, 1932; Sprow & Prausnitz, 1966),

$$\sigma = \sigma_i + \frac{kT}{\mathcal{A}_i} \ln \frac{\gamma_i^s x_i^s}{\gamma_i^b x_i^b}, \tag{4}$$

where $\mathcal{A}_i$ is the partial molecular surface area of compound i, γ_i and x_i are the activity coefficient and mole fraction of species i in each phase of the mixture, and superscripts "s" and "b" refer to the surface and bulk phases, respectively, so that $x_i^b = n_i^b / \sum_j n_j^b$, where n_i^b is the amount of molecules of species i in the droplet bulk, and similarly for the surface $x_i^s = n_i^s / \sum_j n_j^s$. Ming & Russell (2001, 2002) solved equation (4) for the surface composition assuming linear dependence, $x_i^s = k_i x_i^b$ (where k_i is a component specific constant), between surface and bulk mole fractions, while Topping et al. (2005, 2007) solved it iteratively for each compound using the condition $\sum_i x_i^s = 1$ to retrieve σ and surface composition $\{x_i^s\}$. Cai and Griffin (2005) presented a numerical scheme connecting solution of equation (4) under the same condition with mass balance in the form $n_i^s + n_i^b = n_i^t$, where superscript "t" refers to the total amount of component i, to calculate the bulk-surface partitioning within a droplet. For simplicity, they neglected the contribution of inorganic species to the water activity and calculated γ_w for a pseudo-binary organic-water mixture. The partial molecular area $\mathcal{A}_i$ is typically replaced in equation (4) by the molecular area of pure i, although evaluated x_i^s are known to be sensitive to this choice (Topping et al., 2007). In most atmospheric applications, equation (4) is used only to estimate the surface tension of a mixed droplet, utilizing, for example, group contribution methods for obtaining the relevant activity coefficients.

In the limiting cases of either a negligibly water-soluble surfactant or strongly surface avoiding ionic species, complete liquid-liquid phase separation (LLPS; Freedman, 2017) of the bulk and surface may occur. In such conditions, droplets may be envisioned to form a core-shell structure with two or more thermodynamically distinct phases. Phase equilibrium conditions then follow from minimization of the free energy (Shiraiwa et al., 2013; Zuend & Seinfeld, 2013). However, LLPS can also lead to other geometries than core-shell structures, for example, partially engulfed organic- and water-rich phases, as was recently inferred from single particle experiments in an optical trap (Stewart et al., 2015). A simple approximation similar to LLPS was proposed by Prisle et al. (2011): Here the surfactant is assumed to form an insoluble (possibly partial mono-) layer on top of the aqueous solution core, while the surface tension is assumed to remain that of pure water, σ_w. This approach is a simple way to emulate the overall response of activating droplets to partitioning of strong surfactants, as observed in both laboratory experiments and results from more comprehensive models (Prisle et al., 2010). A similar approach was also used by Ruehl and Wilson (2014), who presented the surface monolayer as a film with 2-D van der Waals EoS: At low surface coverage, the adsorbed film is assumed to be in a "gaseous" state with no interactions between surfactant molecules and a phase transition to a more densely packed or "compressed" film takes place, when the full monolayer forms (Seidl, 2000). A simplified version of this approach with compressed film EoS was described by Ruehl et al. (2016). Ruehl et al. (2016) and Forestieri et al. (2018) also considered finite surface layer with surface tension given by the Szyszkowski-Langmuir equation, equation (3). Several studies (e.g., Ellison et al., 1999; Gill et al., 1983) have employed the description of a droplet with surface adsorbed surfactants as an "inverted micelle," in order to relate droplet surface tension depression to the existence of such an organic layer via surface pressure.

Recently, Ovadnevaite et al. (2017) presented an approach allowing for partial droplet coverage by a fully phase-separated organic-rich layer, similar to that of Prisle et al. (2011). Surface tensions of water- and organic-rich phases are expressed as volume fraction weighted averages of pure component surface tensions, while effects of concurrent bulk-surface partitioning of inorganic salts are neglected. Surface coverage by the organic-rich layer is deduced from the estimated volume of the organic-rich phase and the minimum predefined thickness δ_{min} of the surface layer. If the surface coverage is below a full monolayer, the effective surface tension is calculated as the surface area weighted average of the respective water- and organic-rich phase surface tensions.

There are currently no bulk-surface partitioning models fully based on multilayer adsorption isotherms used in atmospheric aerosol models, although several approaches have been presented to quantify the adsorption of water on mainly insoluble particles using such isotherms (e.g., Henson, 2007; Laaksonen & Malila, 2016; Popovicheva et al., 2008; Sorjamaa & Laaksonen, 2007). The statistical mechanics model presented by Wexler and Dutcher (2013) and Boyer et al. (2017) builds on multilayer adsorption concepts but, in practice, assumes single monolayer adsorption (Boyer et al., 2015): This model includes the amounts of different molecules in the surface and bulk as parameters and can therefore in principle provide information on surface partitioning, given that (experimental) surface tension and information on (droplet) system geometry are known. In some of the kinetic models following the framework of Pöschl et al. (2007), separate adsorption and surface layers are presented based on flux and continuity equations of each species in a given layer.

In this work, we introduce a monolayer model, which shares some of the features presented by Prisle et al. (2011), Ruehl and Wilson (2014), and Ovadnevaite et al. (2017), but is prognostic for both composition and thickness of the surface. In contrast to most other suggested approaches, the present model simultaneously evaluates the surface enrichment or depletion for all species within the droplet.

3. Theory and Computation

We consider an aqueous droplet with an (outer) radius R that can be divided into a surface monolayer of thickness δ and an interior (bulk) with radius $R - \delta$ and apply the following relation between droplet surface tension σ, as a function of bulk composition, and surface composition $\mathbf{x}^s = (x_1^s, x_2^s, \ldots)$:

$$\sigma(\mathbf{x}^b, T) = \frac{\sum_i \sigma_i v_i x_i^s}{\sum_i v_i x_i^s}. \tag{5}$$

Here $\mathbf{x}^b = (x_1^b, x_2^b, \ldots)$ are the bulk mole fractions $n_i^b / \sum_j n_j^b$ of each species i in the droplet, x_i^s are the corresponding surface mole fractions, and v_i and σ_i are the molecular volumes and surface tensions of each pure component i. Equation (5) is an extension of the Laaksonen-Kulmala equation (Laaksonen & Kulmala, 1991), which was previously found to provide a quantitative description of surface compositions for plane and curved surfaces of different alcohol-water mixtures, when compared to both experimental (Raina et al., 2001) and computational (Salonen et al., 2005) observations. We here adopt equation (5) as a semiempirical approximation for the droplet solution surface tension, by regarding the relation as a generalization of the Eberhart (1966) model or, alternatively, as a variation of the equations (13.16) derived for the surface tension of an ideal mixture of different size molecules by Defay et al. (1966). In both cases, equation (5) can be interpreted to give the surface tension of the mixture as the surface volume fraction $v_i x_i^s / \sum_j v_j x_j^s$ weighted average of pure component surface tensions.

The partitioning of molecules is calculated under the constraint of conservation of mass within the droplet, such that for each species i, the partitioning of the total amount of molecules, $n_i^t = n_i^s + n_i^b$, between the bulk and surface phases is resolved.

Specifically, for a spherical aqueous droplet, bulk-surface partitioning is evaluated in terms of the set of bulk $\mathbf{x}^b$ and surface $\mathbf{x}^s$ mole fractions for a given droplet radius R and total composition $\mathbf{n}^t = (n_1^t, n_2^t, \ldots)$. The total amount of molecules in the monolayer $\mathbf{n}^s = (n_1^s, n_2^s, \ldots)$ is evaluated from the volume of the monolayer, $V^s = 4\pi[R^3 - (R - \delta)^3]/3$, where the thickness δ of the surface monolayer is given from the equation:

$$\delta = \left(\frac{6}{\pi} \sum_i v_i x_i^s \right)^{1/3}, \tag{6}$$

which conforms with the weighting factor of equation (5). Assuming here that the monolayer can be described as a liquid phase, with composition distinct from the bulk, mass balance of the surface phase can be expressed as

$$\sum_i n_i^s m_i = \rho(\mathbf{x}^s) V^s, \tag{7}$$

where m_i is the molecular mass of each component i and ρ is the density of a bulk liquid with composition corresponding to that of the monolayer $\rho(\mathbf{x}^s, T)$. Equations (6) and (7) now give the absolute number of molecules in the surface layer corresponding to mole fractions $\{x_i^s\}$ from equation (5).

In the following, we consider both binary and ternary aqueous systems, where component 1 refers to water, component 2 to the (strongest) surfactant in the solution, and a possible component 3 to a general solute, for example, a weaker surfactant or a salt. For simplicity, we here denote component 3 as "salt."

For each droplet radius R, (total) volumetric solute concentrations C_2^t and C_3^t are determined from a prescribed solute composition, that is, the total number of solute molecules n_2^t and n_3^t, which are typically obtained from a given size, shape, and composition of the dry particle serving as condensation nucleus for the droplet. The total number of water molecules in the droplet is determined from the conservation of mass

$$n_1^t = \frac{4\pi\rho(\mathbf{x}^b(n_1^t), T)R^3}{3m_1} - \frac{n_2^t m_2 + n_3^t m_3}{m_1}, \tag{8}$$

where $\rho(\mathrm{x}^b, T)$ is the density of a mixture corresponding to the droplet bulk.

As it is not possible to directly solve equation (5) for all surface mole fractions with more than one independent mole fraction, we proceed via pseudo-binary approximations. Considering the droplet as a pseudo-binary solution of salt water (subscript "13") and surfactant (subscript "2"), equation (5) reduces to

$$\sigma(x_{13}^b, x_2^b) = \frac{\sigma_{13} v_{13} x_{13}^s + \sigma_2 v_2 x_2^s}{v_{13} x_{13}^s + v_2 x_2^s}, \tag{9}$$

where $x_{13}^b = 1 - x_2^b = x_1^b + x_3^b$ and $x_{13}^s = x_1^s + x_3^s$ are the salt water component surface and bulk mole fractions. The bulk-surface partitioning of undissociated salt is evaluated from the binary version of equation (5) using the corresponding pseudo-binary bulk and surface salt mole fractions $\tilde{x}_3^b = x_3^b/(x_1^b + x_3^b)$ and $\tilde{x}_3^s = x_3^s/(x_1^s + x_3^s)$, that is, the mole fractions for the same droplet when neglecting the contribution of surfactant:

$$\sigma_{13}(\tilde{x}_3^b, T) = \frac{\sigma_1 v_1 (1 - \tilde{x}_3^s) + \sigma_3 v_3 \tilde{x}_3^s}{v_1 (1 - \tilde{x}_3^s) + v_3 \tilde{x}_3^s}. \tag{10}$$

In equation (10), σ_{13} is analogously the surface tension of the binary water-salt mixture, for which the effective average molecular volume is approximated as

$$v_{13} = \frac{\tilde{x}_1^b m_1 + \tilde{x}_3^b m_3}{\rho_{13}(\tilde{x}_3^b, T)}. \tag{11}$$

Here $\rho_{13}(\tilde{x}_3^b, T)$ is the density of the binary water-salt mixture as a function of the pseudo-binary mole fractions. We can then solve equation (10) for $\tilde{x}_3^s$ and $\tilde{x}_1^s = 1 - \tilde{x}_3^s$, and the surface mole fraction of surfactant in the ternary solution can now be solved from equation (9) using equation (11), as

$$x_2^s = \frac{(\sigma_{13} - \sigma(\mathbf{x}^b, T)) v_{13}}{\sigma(\mathbf{x}^b, T)(v_2 - v_{13}) - (\sigma_2 v_2 - \sigma_{13} v_{13})}. \tag{12}$$

Finally, the ternary surface mole fractions of salt and water are the given as the surface mole fraction of salt water multiplied by the contribution of salt and water to the surface phase, that is, the pseudo-binary mole fractions:

$$x_1^s = (1 - x_2^s)\tilde{x}_1^s, \quad \text{and} \tag{13}$$

$$x_3^s = (1 - x_2^s)\tilde{x}_3^s. \tag{14}$$

Surfactants can form micelles in solutions where the surfactant concentration exceeds the so-called critical micelle concentration (CMC) for the system in question. At this point, the slope of the surface tension concentration adsorption isotherm changes dramatically. For droplet solutions where the surfactant bulk concentration exceeds the CMC ($x_2^b \geq x_{2,\mathrm{CMC}}$), we here assume that $\sigma(\mathbf{x}^b) = \sigma_{\mathrm{CMC}}$ and apply the following approximations

$$x_2^s = 1, \quad \text{and} \tag{15}$$

$$x_1^s = x_3^s = 0. \tag{16}$$

Consequently, formation of pure monolayer with a surfactant surface mole fraction of unity, $x_2^s = 1$, is assumed whenever $x_2^b \geq x_{2,\mathrm{CMC}}$. When the surface tension of the pure surfactant is not known, it is here assumed to be equal to the surface tension of the corresponding aqueous solution at the CMC, $\sigma_2 = \sigma_{\mathrm{CMC}}$, in which case equations (15) and (16) also follow directly from equation (5). In this formulation, the model therefore does not treat micelle formation explicitly. This is similar to other existing approaches (e.g., Cai & Griffin, 2005; Li et al., 1998; Prisle et al., 2010), and in general, more work is needed for a comprehensive treatment of micelle forming systems in atmospheric droplets.

The outlined approach generalizes readily to mixtures with an arbitrary number of compounds by analogously singling out each solute iteratively: For example, if the strongest surfactant in a quaternary system is still the component 2, we first consider system of component 2 and pseudo-component 134, after which the pseudo-component 134 is further split into components, say, 3 and 14.

The procedure outlined in equations (8)–(14) for solving equation (5) is however not readily linearized for a computationally efficient solution. Instead, we solve the system in a two-step iterative manner (in case of ternary systems discussed here) via equations (5) and (6) for the number of molecules in the surface layer $\sum_i n_i^s$ and the number of molecules in the droplet bulk $\sum_i n_i^b = \sum_i (n_i^t - n_i^s)$, respectively. The two key parameters controlling this process are the convergence criterion, given, for example, in terms of bulk mole fractions or surface tension and the iteration step length. The initial guess $\mathbf{x}_0^b$ for bulk mole fractions, and thus also for the droplet surface tension $\sigma_0 = \sigma(\mathbf{x}_\mathbf{0}^\mathbf{b})$, is given using the total composition of the droplet, $\{x_i^t = n_i^t / \sum_j n_j^t\}$. If the chosen convergence criterion is too loose, or the iteration step length too short, this can lead to a numerical solution underpredicting the extent of bulk-surface partitioning of surfactant (overpredicting x_2^b) and underestimating surface tension. Conversely, if the convergence criterion is too tight, or the iteration step length too long, no solution may be found. These parameters are specific to each studied system, depending on the sensitivity of the surface tension parametrization on bulk mole fractions (see the supporting information S1 for further details), and have to be sought and optimized separately for each case.

4. Results and Discussion

In the following, we first present predictions of the monolayer partitioning model for two binary systems, water-*n*-butanol and water-sodium dodecyl sulfate (SDS), and then for ternary aqueous mixtures of SDS or succinic acid (SCA), respectively, with sodium chloride (NaCl). Experimental input data for the model calculations have obtained from the literature, in the form of pure compound and composition-dependent solution surface tensions and densities. Surface tension relations are used in equation (5) and its derivates equations (9) and (10). Density relations are used for obtaining molar volumes v_i used in equations (9) and (11) and their derivates and in the mass conservation relations equations (7) and (8). A detailed description of the thermodynamic input data used in the calculations is given in supporting information S1. Monolayer model results are compared to predictions with the Gibbsian model of Prisle et al. (2010; results consistently shown in red), as well as experimental data from literature.

Figure 1 presents predictions for water-*n*-butanol mixtures with three different total volumetric concentrations of *n*-butanol, $C_{\mathrm{butanol}} = C_{\mathrm{butanol}}^t$, in the droplet (in following, all reported concentrations refer to the total concentrations within the droplet). Droplet surface and bulk mole fractions of *n*-butanol are given in Figures 1a and 1b. For the nonisotropic surfactant solutions, the values of x_{butanol}^s and x_{butanol}^b are generally different, reflecting the difference in composition between the surface and bulk phases arising from surface activity. It is clear from Figure 1 that *n*-butanol is enriched in the surface, compared to the bulk ($x_{\mathrm{butanol}}^s > x_{\mathrm{butanol}}^b$), at all droplet sizes and concentrations. Both surface and bulk mole fractions of *n*-butanol decrease with decreasing droplet radius, due to the change in partitioning induced by the increasing relative

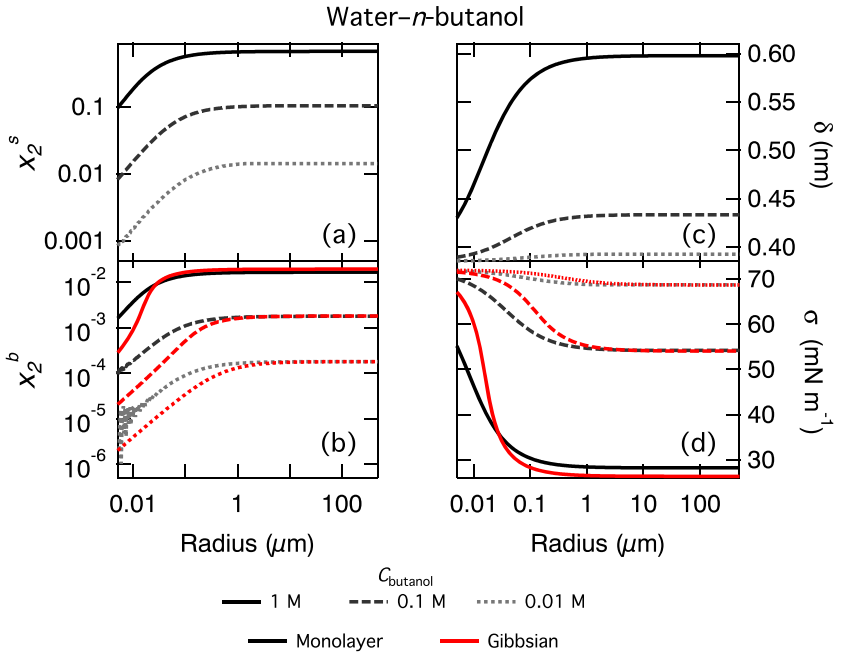

Figure 1. Monolayer partitioning model results for water-*n*-butanol mixtures at 298.15 K with total *n*-butanol concentrations 0.01 (dotted), 0.10 (dashed), and 1.00 M (full lines) as functions of droplet size. (a) Surface and (b) bulk mole fraction of *n*-butanol, (c) surface thickness, and (d) droplet surface tension. In (b) and (d), corresponding results from the Gibbsian partitioning model of Prisle et al. (2010, red lines) are included for comparison.

volume of the butanol-rich surface phase, with respect to the bulk volume. As a consequence, the predicted surface enhancement factor of *n*-butanol (not shown), given by the ratio x^s/x^b of *n*-butanol mole fractions in the surface layer and in the droplet bulk, varies between 40 and 100 and increases with the decreasing total *n*-butanol concentration and decreasing droplet size.

The numerical noise apparent in the calculated bulk mole fractions can be seen for all the systems studied (in Figures 1, 3, and 4) and occurs for smaller droplet sizes and at the highest surfactant concentrations when $x^b_{\mathrm{sft}} \sim 1/(n^b_w + n^b_{\mathrm{sft}} + n^b_{\mathrm{salt}})$. This can be considered as the lower limit for the model uncertainty in bulk composition, as it roughly corresponds to the addition or extraction of a single (surfactant) molecule from the droplet bulk phase.

The surface thickness δ decreases with surface mole fraction of surfactant according to equation (6). This is clearly reflected in Figure 1c, where the surface thickness decreases with both decreasing total *n*-butanol concentration and droplet size, in a similar trend as observed for x^s_{butanol} in Figure 1a. At droplet sizes above approximately 1 μm, δ tends to the values for corresponding bulk systems (with planar surfaces). For larger C_{butanol} and x^s_{butanol}, the surface thickness tends toward the thickness of a full *n*-butanol monolayer, 0.66 nm (for predicted pure compound monolayer thicknesses of all studied surfactants and water, see Table 2).

The surface tension σ in Figure 1d increases with decreasing droplet size, due to the decrease in *n*-butanol bulk mole fraction x^b_{butanol}. The droplet surface tension is parametrized as function of droplet bulk composition and tends toward the value for pure water as bulk depletion of surfactant molecules from surface partitioning becomes more pronounced with the increasing surface-bulk volume ratio of decreasing droplet sizes. For larger droplets, σ reaches the values for corresponding planar surfaces at each total concentration around 1 μm. For all properties shown in Figure 1, changes from bulk solution (planar surface) properties start to appear for droplets in the submicron range and become more pronounced with decreasing droplet radius.

In Figures 1b and 1d, *n*-butanol bulk mole fraction and surface tension predicted for this work with the Gibbsian partitioning model of Prisle et al. (2010) are given for comparison. At each total *n*-butanol concentration, the onset of surface tension increase from the planar surface-bulk values with decreasing droplet sizes occurs in smaller droplets with the monolayer droplet model, compared to the Gibbsian approach. This means that

Table 2
Limiting Surface Thickness δ for Water and Pure Surfactant Monolayers From Equation (6)

Compound	δ (nm)
Water	0.39
SCA	0.63
n-Butanol	0.66
SDS	0.93

Note. SCA = succinic acid; SDS = sodium dodecyl sulfate.

the droplet surface tension remains reduced, compared to pure water, down to smaller droplet sizes in the monolayer model predictions. This is due to the different approaches to evaluating bulk-surface partitioning in the two model frameworks. In our monolayer model, only a finite amount of (relatively large, compared to water) surfactant molecules can be accommodated into a surface monolayer with finite volume (thickness δ), as given by equation (6). This volume limitation restricts remaining surfactant molecules at concentrations above this surface "saturation" limit to the droplet bulk, thereby increasing the bulk mole fraction x^b_{sft} and decreasing the droplet surface tension, which is parametrized in terms of bulk phase composition. The monolayer model predictions are therefore sensitive to the definition of surface layer thickness, imposing the limitation on the absolute extent of surface partitioning. In the Gibbsian model, partitioning occurs with respect to a dividing surface which has no volume and thus imposes no similar physical restriction on the extent of the surface adsorption, as long as at least one of the remaining droplet components can attain a corresponding negative surface excess. The evaluated surface excess of surfactant can therefore be considerable in the Gibbsian droplet model, which generally predicts larger surface excesses and smaller bulk concentrations, resulting in higher droplet surface tensions, at a given droplet size and total composition, compared to our present monolayer model. The effect is especially pronounced for intermediate droplet sizes with concentrations in the surface tension transition region between pure water and bulk system values. This difference between the monolayer and Gibbsian models is a general feature apparent for each of the four aqueous droplet systems studied here, as seen Figures 3, 4, and 6 in the following.

In Figure 2 (see also Figure 5 of Raina et al., 2001), predictions of surface thickness (top) and surface mole fraction (bottom) as functions of bulk mole fraction with the present monolayer model are compared to measurements for planar surfaces (bulk systems) of water-*n*-butanol mixtures. Measurements are made at room temperature using different experimental methods, including (i) neutron reflection (Li et al., 1996), (ii) mass spectrometric probing of molecular clusters, presumably in equilibrium in the headspace above a liquid surface (Raina et al., 2001), and (iii) analysis of experimental surface tension data based on Gibbs' adsorption equation (equation (2); Li et al., 1996). Together with (iv) X-ray photoelectron spectroscopy (XPS; Walz et al., 2016), these methods have been used to probe the composition and thickness of water-*n*-butanol surfaces. There are quantitative differences between the results obtained from the different measurements; however, considering the complex nature of the experiments, the qualitative agreement (numerically within about a factor of three) is quite reasonable. The quantitative differences may arise from variations in measurement precision and accuracy but also that the various methods probe the surface to different extent. The determined total amount of *n*-butanol in the surface layer is convoluted by method-dependent assumptions regarding the surface thickness or volume producing the observed signal. Thus, the actual observable is the product of the surface concentration—or, in case of neutron reflection experiments, the surface concentration dependent scattering length density—and the probed surface volume, which for planar surfaces is proportional to the surface thickness. This was recently highlighted by Toribio et al. (2018), together with other potential challenges to obtaining quantitative surface concentrations from XPS measurements on a 20-μm liquid microjet (Walz et al., 2015, 2016). Toribio et al. (2018) reported surface enrichment factors for aqueous *n*-butanol, modeled from a statistical mechanics based surface model (Boyer et al., 2015; Wexler & Dutcher, 2013), which are of similar magnitude albeit somewhat smaller, compared to the present monolayer model. Curiously, Toribio et al. (2018) find similar discrepancies of about a factor of 3 between their model predictions and experimental XPS-derived surface concentrations of aqueous alcohols (Walz et al., 2016). This comparison was however done for *n*-butanol concentrations an order of magnitude higher than in the studies compared in Figure 2.

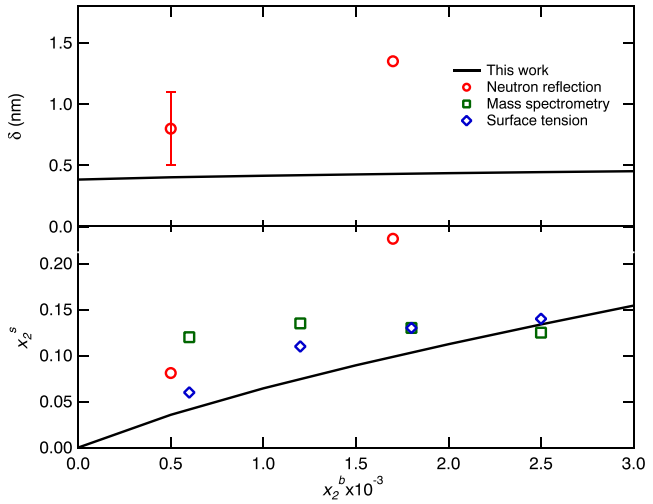

Figure 2. Comparison of predicted surface thickness and *n*-butanol surface mole fraction for water-*n*-butanol mixtures from the monolayer model, to experimental values from neutron reflection (circles), and Gibbs' adsorption equation based analysis of experimental surface tension data (diamonds; Li et al., 1996) as recalculated by Bermúdez-Salguero and Gracia-Fadrique (2015) assuming $\delta = 0.7$ nm, and from mass spectrometry (squares; Raina et al., 2001).

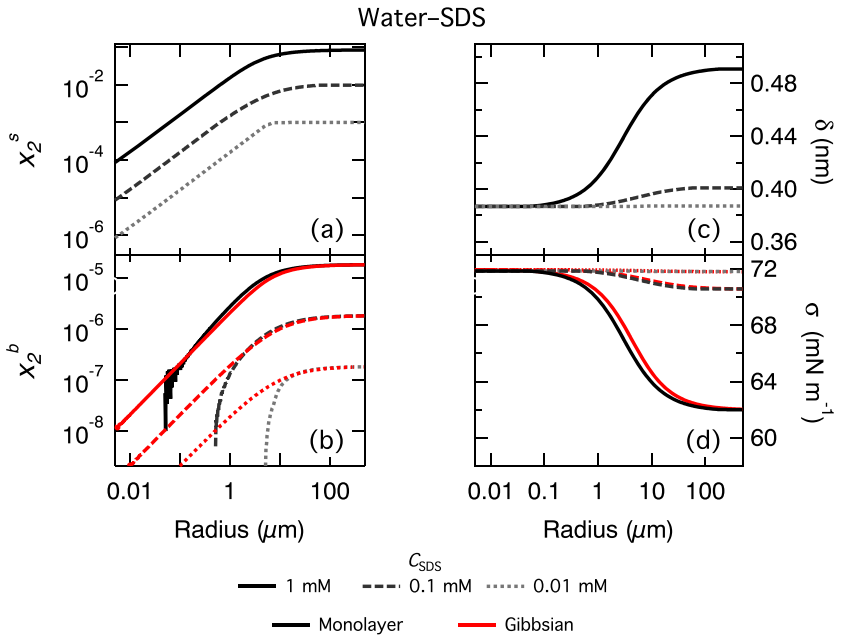

Figure 3. Same as Figure 1 for water-SDS mixtures, with total SDS concentrations 0.01 (dotted), 0.10 (dashed), and 1.00 mM (full lines). SDS = sodium dodecyl sulfate.

Considering the neutron reflection data, Bermúdez-Salguero and Gracia-Fadrique (2015) have noted a thermodynamic inconsistency in the values calculated by Raina et al. (2001; corrected values are given in Figure 2), which highlights a yet another potential source of uncertainty.

Wyslouzil et al. (2006) used small angle neutron scattering to quantify the structure of water-*n*-butanol droplets formed by adiabatic expansion at 235 K. As their measurements were made at significantly lower temperatures, results are not shown together with the other studies in Figure 2. For 10-μm droplets, Wyslouzil et al. (2006) inferred a core-shell structure with a 0.42-nm-thick pure *n*-butanol surface and resulting surface enrichment factor 34 for the given total *n*-butanol concentration. This is slightly above the saturation limit (in the solubility gap) of water-*n*-butanol mixtures and model results depicted in Figure 1 and thus in line with our presented monolayer model, although it is not possible to directly compare these results to our model predictions, due to lack of relevant thermodynamic data for performing model simulations at those low temperatures.

In Figure 3, monolayer model results are presented for water-SDS mixtures with three different total concentrations C_{SDS}. SDS is a significantly stronger surfactant than *n*-butanol (see supporting information S1 for further details on material properties used in the calculations), and total droplet concentrations in Figure 3 are three orders of magnitude lower than those presented for *n*-butanol in Figure 1. In Figures 3a and 3b, SDS surface and bulk mole fractions, x^s_{SDS} and x^b_{SDS}, are given as functions of droplet size for each C_{SDS}, and the corresponding droplet surface thickness and surface tension values are presented in Figures 3c and 3d. Results for aqueous SDS droplets are qualitatively similar to those for *n*-butanol, but as expected, the bulk-surface partitioning response of SDS to increasing surface-bulk volume ratio with decreasing droplet size is much stronger. Changes in both surface and bulk phase composition, and corresponding surface thickness and surface tension, from the planar surface (infinite droplet size) limit start to occur already for droplets just below 10 μm. In particular, total SDS concentrations that result in a significant decrease of surface tension (e.g., by 10 mN/m) in the planar surface limit are essentially completely depleted from the droplet bulk by partitioning of SDS into the surface layer for droplets with radii smaller than about 0.1 μm. As a result, the droplet surface tension is the same as for pure water. This behavior represents the main underlying assumption of the simple representation presented by Prisle et al. (2011) and explains the good performance of their model for aqueous SDS droplets.

In contrast to results for *n*-butanol-water systems, predictions for SDS are qualitatively very similar between the monolayer and Gibbsian partitioning models, as seen from the evaluated bulk compositions and surface

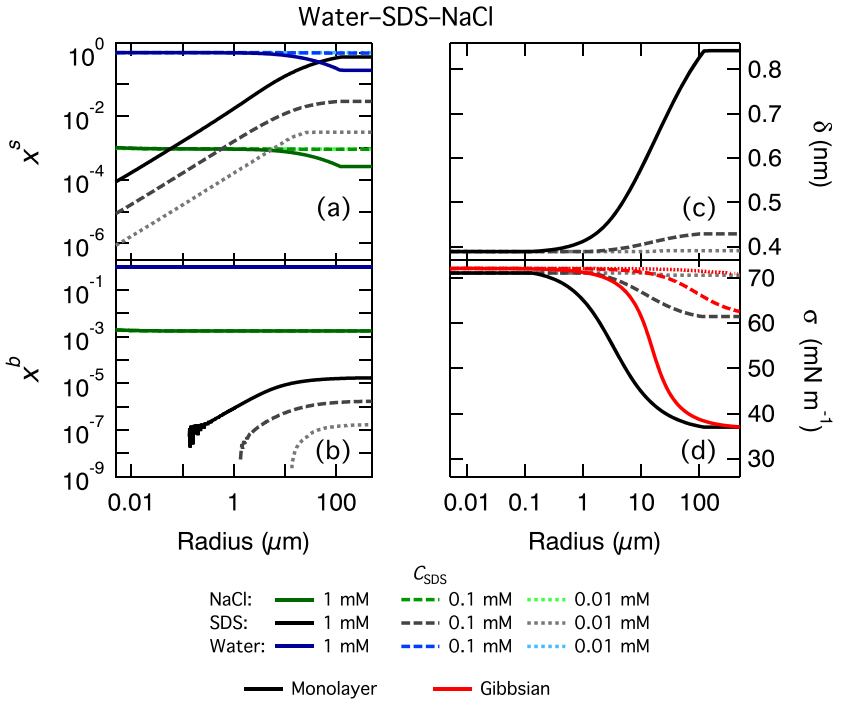

Figure 4. Monolayer partitioning model results for ternary water-SDS-NaCl mixtures at 298.15 K with total SDS concentrations of 0.01 (dotted), 0.10 (dashed), and 1.00 mM (full lines) and constant NaCl total concentration 0.1 M, corresponding to relative solute mixing ratios of 10^{-4}, 10^{-3}, and 10^{-2}, respectively. Size-dependent (a) surface and (b) bulk mole fractions of SDS (black), NaCl (green), and water (blue), (c) surface thickness, and (d) surface tension of the droplet. Results from the Gibbsian partitioning model of Prisle et al. (2010, red lines) for the droplet surface tension are also included in (d) for comparison. SDS = sodium dodecyl sulfate.

tensions in Figures 3b and 3d, respectively. This is partly a consequence of the lower total concentrations considered. Furthermore, SDS is a sufficiently strong surfactant that the bulk phase becomes almost completely depleted at small droplet sizes from partitioning into the surface monolayer. In the Gibbsian framework, partitioning occurs according to the adsorption equilibrium, and there is always a fraction of surfactant left in the bulk, as seen in Figure 3b. This creates similar conditions in the two frameworks for the droplets in question.

Figure 4 present results for ternary water-SDS-NaCl mixtures with the same total SDS concentrations as in Figure 3 and a constant total NaCl concentration of 0.1 M, as functions of droplet size. The monolayer model evaluates bulk-surface partitioning of all molecular species in the droplet, and consequently, the surface and bulk mole fractions, x^s and x^b, of water and undissociated SDS and NaCl are all given in Figures 4a and 4b. Surface partitioning of SDS results in qualitatively very similar behavior of both x^s_{SDS} and x^b_{SDS} (green lines) in ternary solutions, as seen for binary aqueous SDS in Figure 3. At the highest total SDS concentration (1 mM, full lines), nearly a pure surfactant monolayer is formed ($x^s_{SDS} \sim 1$, full black line) at large droplet radii (in the planar limit), and both water and NaCl are depleted from the surface layer, as indicated by decreasing surface fractions x^s_w (blue, full line) and x^s_{NaCl} (green, full line) in Figure 4a. This depletion, however, has no significant effect on the corresponding water and NaCl bulk mole fractions, x^b_w (blue, full line) and x^b_{NaCl} (green, full line), in Figure 4b, due to the much smaller surface-bulk volume ratio of solutions in the planar limit. For smaller droplets, water and NaCl surface fractions are unchanged across droplet sizes and between different total SDS concentrations, due to smaller partial surface coverage of SDS.

The depletion of water and NaCl from the surface layer causes greater responses in both surface layer thickness and surface tension of ternary droplets shown in Figures 4c and 4d, respectively, compared to binary aqueous SDS solutions. For the two lower C_{SDS}, where $x^s_{SDS} << 1$, δ is comparable to the corresponding binary cases. At the highest C_{SDS}, the surface thickness increases significantly as water and NaCl are depleted from the surface at larger droplet sizes. Here the absolute surface thickness is almost doubled compared to the

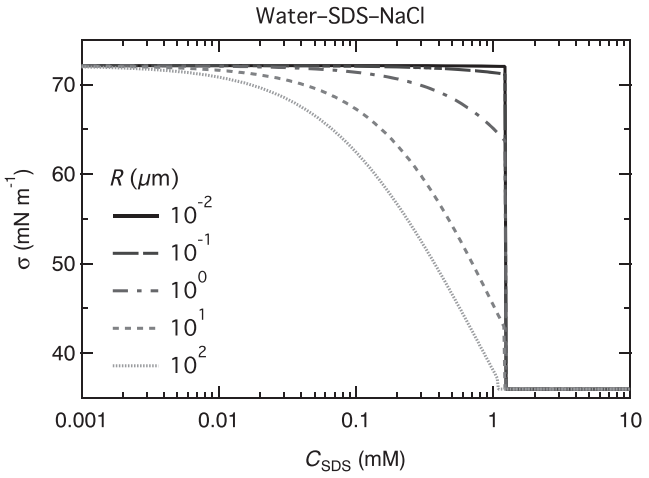

Figure 5. Surface tension predicted with the monolayer partitioning model for different droplet sizes, as a function total concentration of SDS in ternary water-SDS-NaCl mixtures at 298.15 K and with a total NaCl concentration of 0.1 M. SDS = sodium dodecyl sulfate.

salt-free binary case (Figure 3). This follows from the inverse relationship between surface tension and surface thickness given by equations (5) and (6), since the molecular volume assumed for SDS is significantly larger than those of water and NaCl (see supporting information S1).

The SDS surface mole fraction and droplet surface thickness begin to decrease from the planar surface limit already below droplet radii about an order of magnitude larger (100 μm) than for binary aqueous SDS. This reflects the significant surface activity of SDS, which is further enhanced by salting out effects of NaCl on SDS surface partitioning. The corresponding SDS bulk mole fractions and resulting droplet surface tensions are much less sensitive to this effect, showing only slightly increased sensitivities to droplet size, compared to the binary solutions in Figure 3. The absolute surface tension decrease is however significantly greater for the ternary solutions, both in planar limit and for droplet sizes in the surface tension transition range, both as a consequence of salting out. The current framework of the monolayer model does not consider dissociation of ions and therefore also not the so-called "common ion effect" that may affect the speciation of ionic surfactants and salts in solution due to an impact of a common ion, here Na^+, on cosolvation properties (Raatikainen & Laaksonen, 2011; Topping, 2010). However, the existence of the common ion effect is still a matter of debate; Prisle, Ottosson, et al. (2012) and Öhrwall et al. (2015) found no evidence for salting out specifically due to common Na^+ ions in direct observations of aqueous surfaces composing selected sodium carboxylate mixtures with various inorganic salts using synchrotron-based XPS.

Droplet surface tensions from the Gibbsian model are included for comparison in Figure 4d; the corresponding bulk mole fractions have been omitted from Figure 4b for clarity. In contrast to the binary case in Figure 3b, monolayer model predicted SDS bulk mole fractions are now significantly higher, compared to the Gibbsian model (not shown). As surface partitioning of SDS is enhanced by salting out in the ternary mixtures, monolayer volume restrictions on partitioning become more evident. The monolayer model therefore predicts significantly lower surface tensions for droplets in the transition size range, as seen in Figure 4d. For the ternary systems, a minor opposing effect on surface tension may occur simultaneously due to surface depletion of the inorganic salt, causing a slight relative increase in surface tension. However, the significant decrease in overall ternary surface tension, compared to binary aqueous SDS droplets, shows that this effect is not major for these strong surfactant solutions.

Figure 5 shows the dependency of predicted surface tension on total SDS concentration for ternary water-SDS-NaCl droplets of various sizes. The smaller droplets display increasingly steep transitions to surface saturation, as seen from constant reduced surface tension $\sigma = \sigma_{CMC,SDS}$, with increasing concentration of SDS: The smallest droplets (10 nm) undergo nearly a step change in surface tension reminiscing the phase transition between gaseous and compressed surface layers described by Ruehl and Wilson (2014). As droplet sizes increase, surface tension concentration dependencies change gradually to eventually resemble the regular bulk behavior observed for macroscopic solutions in case of the largest droplets (100 μm). This variation in surface tension concentration isotherms with droplet size stems mainly from the varying influence of surfactant bulk phase depletion from bulk-surface partitioning in droplets with different sizes and surface-bulk volume ratios. A contributing factor is the approximation of pure surfactant surface tension with that of the aqueous mixture at the CMC and the assumption of a pure surfactant monolayer for concentrations at and above the CMC. This simplification exaggerates the transition from a saturated, pure SDS surface layer to a mixed surface layer corresponding to low SDS bulk concentrations, according to equation (5). The effect is especially pronounced at small droplet sizes, where only a few molecules of SDS in the droplet bulk can strongly influence the estimated surface tension. The change in surface tension concentration relation is accompanied by a small but notable shift in apparent CMC to higher concentrations in the smaller droplets. In Figure 5, the CMC is 1.09 mM for a 100-μm droplet and gradually increases to 1.24 mM for 10-nm droplets. The CMC for the corresponding bulk system is 1.05 mM. Due to the logarithmic concentration scale, the effect is barely visible for the water-SDS-NaCl system in Figure 5. It may be even more significant for stronger surfactants, just as the atmospheric implications of even small changes in CMC for aqueous droplets could prove to be important.

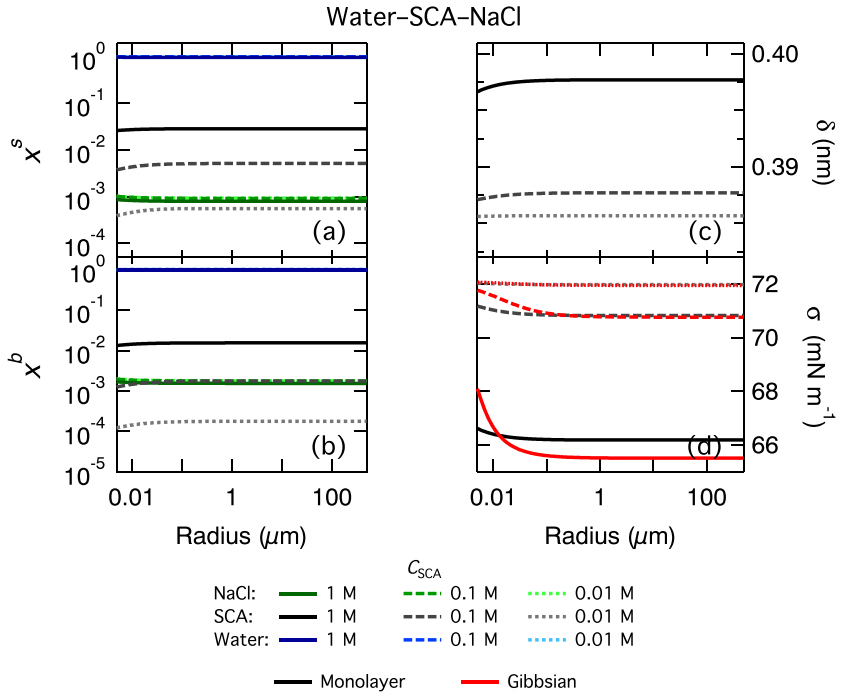

Figure 6. Same as Figure 4 for water-SCA-NaCl solutions, with total SCA concentrations of 0.01 (dotted), 0.10 (dashed), and 1.00 M (full lines) and a fixed total concentration of 0.10-M NaCl, corresponding to relative solute mixing ratios of 0.10, 1.0, and 10, respectively. SCA = succinic acid.

Monolayer model results for more atmospherically relevant water-SCA-NaCl mixtures with three different total SCA concentrations and a constant total NaCl concentration of 0.1 M are presented in Figure 6. Surface and bulk mole fractions of each droplet component are again shown in Figures 6a and 6b, and the corresponding surface layer thickness and droplet surface tension are given in Figures 6c and 6d. SCA is a weaker surfactant than SDS (see supporting information S1), and predicted size dependencies in droplet properties due to bulk-surface partitioning are correspondingly much weaker, as was also noted when comparing binary solutions of SDS and *n*-butanol.

For three orders of magnitude higher C_{SCA} than considered for ternary SDS mixtures, partitioning effects on SCA mole fractions, x^s_{SCA} and x^b_{SCA} (black lines), are only manifest for the smallest droplet sizes below 10–100 nm, as seen in Figures 6a and 6b, respectively. This is reflected in the corresponding surface thickness and surface tension in Figures 6c and 6d, which resemble the planar limit (bulk) values for all but the smallest droplet sizes.

Comparing surface tensions predicted with the monolayer and Gibbsian models in Figure 6d, an interesting feature is the deviation of the two model predictions for the largest C_{SCA}, when approaching the planar surface limit. This behavior was also seen for *n*-butanol in Figure 1 but to a lesser extent than here for water-SCA-NaCl. It is unlikely that such an effect could be due to fundamentally different surface thermodynamics between the monolayer and Gibbsian models, as deviations are otherwise seen in the surface tension transition region for intermediate droplet sizes. Instead, a more likely explanation are different assumptions regarding aqueous solution ideality in the two models. The Gibbsian models in general require explicit input of droplet component activities, which can be extremely difficult to obtain with high reliability over the entire relevant range of droplet (bulk) compositions $\mathbf{x}^b$. Due to lack of explicit activity data, the Gibbsian model of Prisle et al. (2010) is here run assuming ideal solution behavior for the ternary water-SCA-NaCl system, in the terms of unity mole fraction based activity coefficients and partial molecular volumes of individual compounds in the liquid mixture which are independent of the solution composition. For the water-*n*-butanol mixture, on the other hand, activity coefficients needed for the evaluation of the Gibbs' adsorption equation were obtained from van Laar fits presented in the literature, see supporting information S1 for details. The monolayer model implicitly accounts for droplet solution nonideality by using experimental surface tension and density concentration relations in equation (5) and to evaluate v_i. The treatments of droplet component activities in the Gibbsian

model may therefore lead to differences between predictions with the two surface frameworks and greater differences for the case of ternary SCA where nonideal activities are not treated at all in the Gibbsian model.

The Gibbsian model furthermore does not account for any bulk-surface partitioning of salt with respect to water, which likely contributes to enhancing the effect for ternary water-SCA-NaCl, compared to binary water-*n*-butanol. However, as the monolayer model does not predict any significant size-dependent bulk-surface partitioning of either SCA or NaCl in Figures 6a and 6b, salt partitioning cannot be the main reason for the deviation of planar surface tensions between models seen in Figure 6d. As this factor is explicitly accounted for in the monolayer model, the extent to which each of these contributions to surface thermodynamics affect the partitioning estimate is a subject of future studies.

Werner et al. (2014, 2016) recently studied surfaces of aqueous SCA with and without added salts, using synchrotron radiation-based XPS in combination with molecular dynamics simulations. Experiments were made with the same setup as used by Walz et al. (2015, 2016), and direct comparison between experimental and modeled results and our monolayer model is affected by the same issues as pointed out by Toribio et al. (2018) for water-alcohol mixtures. Nevertheless, surface enrichment factors for SCA, x^s_{SCA}/x^b_{SCA}, predicted here from the monolayer model are close to the lower range of the corresponding C^s_{SCA}/C^b_{SCA} values reported by Werner et al. (2014, 2016). Values are expected to differ somewhat, as the ratios are taken for different (mole fraction vs. volumetric) quantities; however, with the same surface thicknesses, these differently derived enrichment factors should agree in the planar limit. Furthermore, the surface thickness of 0.4 nm estimated by Werner et al. (2014) from molecular dynamics simulation for the water-SCA mixture is very close to our predicted values (between 0.38 and 0.40 nm) given in Figure 6 for the water-SCA-NaCl mixture. We especially note that these different estimates are completely independent. Surface thicknesses inferred by Ruehl and Wilson (2014) for dicarboxylic acid monolayers (0.39 nm for adipic acid and 1.02 nm for pimelic acid on SCA-ammonium sulfate particles) are also in this same range.

Ruehl et al. (2016) and Ovadnevaite et al. (2017) in their droplet models assumed much lower surface thicknesses of 0.07–0.21 and 0.16–0.30 nm, respectively, corresponding to one or two carbon-carbon bond lengths, for a dicarboxylic acid surrogate of atmospherically relevant surfactants. These values are also lower than the molecular length of the organic surfactants in question and thus imply near-parallel orientation of surfactant molecules at the surface layer, in contrast to the head-tail perpendicular orientation to the surface commonly assumed for concentrated solutions of linear surfactants (Adamson & Gast, 1997). Experimental observations have been reported of parallel-oriented surfactant molecules at plane aqueous surfaces at low concentrations of some surfactant solutions, while a "gaseous-to-compressed" transition takes place at higher concentrations, preceded by reorientation of surfactant molecules perpendicular to the surface (Prisle, Ottosson, et al., 2012; Richmond, 2001; Walz et al., 2016). Parallel orientation of surfactant molecules with respect to the water surface will yield a much greater molecular footprint in the surface. This in turn would imply a smaller maximum reduction in estimated surfactant bulk mole fraction due to bulk-surface partitioning, and correspondingly higher surface tension, compared to the version of the monolayer model presented here.

In calculating cloud droplet activation for model surfactant aerosol systems, Petters and Petters (2016) found droplet surface excesses corresponding to up to 15 monolayers, using the approximate Gibbsian approach of Raatikainen and Laaksonen (2011). While greater surface enhancements of surfactant may be expected in the Gibbsian surface framework, where surface partitioning is not restricted by volume limitations of the surface phase, this directly contradicts the assumptions of the Szyszkowski-Langmuir surface tension model used for the calculations. Indeed, in most cases, Petters and Petters (2016) found that restricting the surface excess corresponding to much lower 1.5 monolayers improved their model predictions.

The monolayer surface framework can readily be included in a Köhler model to account for bulk-surface partitioning in predictions of cloud droplet activation, analogously to previous work with Gibbsian models (Forestieri et al., 2018; Prisle et al., 2010; Sorjamaa et al., 2004; Topping, 2010). Here, the differences in surface dynamics between the droplet frameworks observed in Figures 1, 3, 4, and 6 may in turn lead to differences in predicted activation behavior of aqueous surfactant droplets. To illustrate this, we consider the case of a 100-nm-diameter dry particle, consisting of 90% by mass SDS and 10% NaCl, for which the Gibbsian model was found by Prisle et al. (2010) to give a good agreement with measurements of critical supersaturation ($SS_c = S_c - 1$). With the conditions used here, the full Gibbsian partitioning model predicts a critical radius (R_c) of 0.24 μm and SS_c of 0.31% from equation (1), together with a surface tension of 62.2 mN/m at the point activation. The simple model of Prisle et al. (2011), where all surfactant is assumed to partition to the

droplet surface, while assuming surface tension of pure water (72.0 mN/m at 298.15 K), yields $R_c = 0.12$ μm and $SS_c = 0.58\%$. Most notably, the critical droplet size predicted by the simple partitioning model yields a surface layer corresponding to 0.35 pure surfactant monolayers, assuming the same limiting value for a full SDS monolayer thickness as given in Table 2. The present monolayer model predicts $R_c = 0.39$ μm and critical supersaturation of 0.18%, with a surface monolayer thickness of 0.48 nm (i.e., half of the pure surfactant monolayer) and droplet surface tension of 55.0 mN/m at activation. Of the three droplet frameworks, the monolayer model in this case predicts significantly higher cloud condensation nuclei activity, a larger critical droplet, and lower droplet surface tension at the point of activation. Although a detailed discussion on these differences is beyond the scope of this work, we note that the presented monolayer model, while allowing for bulk-surface partitioning of all compounds, does give physically reasonable predictions concerning both the nature of the surface layer as well as droplet activation behavior. Detailed results for inclusion of the monolayer model in Köhler predictions for both model surfactant aerosol and atmospherically relevant complex mixtures are presented by Lin et al. (2018).

Finally, we emphasize that when comparing model predictions from approaches based on different treatment of surface thermodynamics, it must be kept closely in mind that the magnitude of evaluated quantities depend inherently on the assumed framework. In particular, the surface excess quantities Γ_i evaluated in the Gibbsian framework are not immediately comparable with the surface mole fractions x_i^s given by the present monolayer or other physical surface layer models. For finite systems like small droplets, we see how this in turn is reflected in different evaluated bulk properties between the frameworks. This is also case for the surface excess free energy, that is, surface tension. Only the total free energy of the droplet (with respect to some reference state) is truly invariant with the choice of thermodynamic framework, as well as with the choice of dividing surface within the Gibbsian model (Rusanov, 1978; Vehkamäki, 2006). Therefore, when considering outputs of different droplet models, or when comparing model predictions with experiments, direct comparison of surface composition, surface enhancements, or surface tension must be done carefully keeping this in mind. In particular, when considering the effect of bulk-surface partitioning on cloud droplet activation by equation (1), this means that differences in predictions with different thermodynamic frameworks must be taken into account simultaneously for both Raoult and Kelvin terms. Currently, direct measurements of droplet surface tensions are highly nontrivial in the micron range and limited to systems above approximately 10 μm in radius (Bzdek et al., 2016). For the systems studied here, surface tensions approach or coincide with the planar limit already at these sizes.

5. Conclusions

We have presented a simple monolayer model for predicting bulk-surface partitioning of especially organic surfactants in aqueous droplets. The model was evaluated for droplets of varying size comprising commonly considered butanol and SDS model surfactants and an atmospherically relevant dicarboxylic acid. The monolayer model is based on an extension of the Kulmala-Laaksonen surface tension model and the principle of mass conservation. It is prognostic for bulk and surface concentrations of all species in the droplet, as well as for the surface monolayer thickness, thus overcoming some of the chief limitations in other recent models (e.g., Ovadnevaite et al., 2017; Prisle et al., 2011; Ruehl et al., 2016). In its current form, the monolayer model does not treat chemical dissociation (electrolytes and hydrolysis) explicitly and therefore cannot predict different surface propensities for dissociated and undissociated species or for the different ions from the same salt or hydrolyzed organic (cf. Pegram & Record, 2006), potentially affecting heterogeneous chemistry at droplet surfaces. The monolayer model predictions agree qualitatively with the Gibbsian droplet model of Prisle et al. (2010) but generally predict higher bulk phase concentrations of surface active species in droplets of the same size and total composition, especially for large surfactant molecules, due to the restricting condition imposed on the extent of surface partitioning by the finite monolayer thickness. For smaller droplets, this condition leads to behavior similar to the compressed-gaseous transitions in surface films described by Ruehl and Wilson (2014).

The real advantage of the monolayer model is that it requires fewer inputs of specific thermodynamic data than other alternatives, for example, droplet models based on the Butler-Sprouw-Prausnitz or Gibbs' adsorption equations. Such required data are often not available for atmospherically relevant mixtures, which remains a major limitation in atmospheric applications of surface partitioning frameworks. In particular, composition-dependent activity relations are extremely challenging to measure directly for sparingly soluble or low volatility solutes and inferences from measured solvent (water) activities via the Gibbs-Duhem relation

fundamentally cannot be extended beyond binary solutions. In contrast, nonideal solution interactions are implicitly included in the monolayer model via experimental, composition-dependent surface tension, and density data, and explicit knowledge of activity coefficients for neither water nor surfactant and salt solutes is required to capture real solution behavior. Although still nontrivial, these properties may be obtained with significant accuracy from well-established and broadly available experimental methods. Furthermore, the presented monolayer model is completely self-contained and requires no tunable parameters in addition to thermodynamic input data. It lends itself readily for inclusion into cloud activation and atmospheric models and provides a viable basis for further development of thermodynamic multilayer models that can also treat micellization and post-CMC droplet behavior explicitly.

Appendix A: Data Sources

Experimental pure substance densities and surface tensions used in the calculations were taken from Wölk and Strey (2001) for water, from Strey and Schmeling (1983) and Ghosh et al. (2008) for *n*-butanol, from Hyvärinen et al. (2006) for SCA, from Kodama and Miura (1972), Persson et al. (2003), and Kumar and Ghosh (2006) for SDS, and from Janz (1980) for NaCl. For binary aqueous mixtures of *n*-butanol, NaCl, and SCA, relations for liquid densities as functions of composition were taken from Dawe et al. (1973), Rowe and Chou (1970), and Hyvärinen et al. (2006), respectively, and for ternary water-SCA-NaCl mixtures from Vanhanen et al. (2008); for other mixtures, ideal solution densities were assumed. Szyszkowski parameters for composition-dependent surface tensions of water-*n*-butanol and water-SDS-NaCl mixtures were taken from Krisch et al. (2007) and Prisle et al. (2010), respectively; for water-SCA-NaCl mixtures, parameters given by Vanhanen et al. (2008) for the surface tension relation presented by Chunxi et al. (2000) were used. Activity coefficients for water-*n*-butanol mixtures were obtained from the compilation of Gmehling and Onken (1977) and in other mixtures assumed to be unity. Further details are given in supporting information S1.

Acknowledgments
This project has received funding from the European Research Council (ERC) under the European Union's Horizon 2020 research and innovation programme, Project SURFACE (grant agreement 717022). The authors also gratefully acknowledge the financial contribution from the Academy of Finland (grants 308238 and 314175). We thank Jack Lin for his assistance on language and layout. Data needed to reproduce calculations given in this article can be found from the supporting information S1.

References

Abdul-Razzak, H., & Ghan, S. J. (2004). Parameterization of the influence of organic surfactants on aerosol activation. *Journal of Geophysical Research*, *109*, D03205. https://doi.org/10.1029/2003JD004043

Adamson, A. W., & Gast, A. P. (1997). *Physical chemistry of surfaces* (6th ed.). New York: Wiley.

Bermúdez-Salguero, C., & Gracia-Fadrique, J. (2015). Gibbs excess and the calculation of the absolute surface composition of liquid binary mixtures. *Journal of Physical Chemistry B*, *119*, 5598–5608. https://doi.org/10.1021/acs.jpcb.5b01436

Bianco, H., & Marmur, A. (1992). The dependence of the surface tension of surfactant solutions on drop size. *Journal of Colloid and Interface Science*, *151*, 517–522. https://doi.org/10.1016/0021-9797(92)90499-C

Boyer, H. C., Bzdek, B. R., Reid, J. P., & Dutcher, C. S. (2017). Statistical thermodynamic model for surface tension of organic and inorganic aqueous mixtures. *Journal of Physical Chemistry A*, *121*, 198–205. https://doi.org/10.1021/acs.jpca.6b10057

Boyer, H., Wexler, A., & Dutcher, C. S. (2015). Parameter interpretation and reduction for a unified statistical mechanic surface tension model. *Journal of Physical Chemistry Letters*, *6*, 3384–3389. https://doi.org/10.1021/acs.jpclett.5b01346

Brüggemann, M., Hayeck, N., Bonnineau, C., Pesce, S., Alpert, P. A., Perrier, S., et al. (2017). Interfacial photochemistry of biogenic surfactants: A major source of abiotic volatile organic compounds. *Faraday Discussions*, *200*, 59–74. https://doi.org/10.1039/C7FD00022G

Butler, J. A. V. (1932). The thermodynamics of surfaces of solutions. *Proceedings of the Royal Society of London A*, *135*, 348–375. https://doi.org/10.1098/rspa.1932.0040

Bzdek, B. R., Power, R. M., Simpson, S. H., Reid, J. P., & Royall, C. P. (2016). Precise, contactless measurements of the surface tension of picolitre aerosol droplets. *Chemical Science*, *7*, 274–285. https://doi.org/10.1039/C5SC03184B

Cai, X., & Griffin, R. J. (2005). Theroretical modeling of the size-dependent influence of surface tension of the absorptive partitioning of semi-volatile organic compounds. *Journal of Atmospheric Chemistry*, *50*, 139–158. https://doi.org/10.1007/s10874-005-2364-2

Chakraborty, P., & Zachariah, M. R. (2011). On the structure of organic-coated water droplets: From "net water attractors" to "oily drops". *Journal of Geophysical Research*, *116*, D21205. https://doi.org/10.1029/2011JD015961

Chunxi, L., Wenchuan, W., & Zihao, W. (2000). A surface tension model for liquid mixtures based on the Wilson equation. *Fluid Phase Equilibria*, *175*, 185–196. https://doi.org/10.1016/S0378-3812(00)00447-7

Daskalakis, V., Charalambous, F., Demetriou, C., & Georgiou, G. (2015). Surface-active organic matter induces salt morphology transitions during new atmospheric particle formation and growth. *RSC Advances*, *5*, 63,240–63,251. https://doi.org/10.1039/c5ra09187j

Dawe, R. A., Newsham, D. M. T., & Ng, S. B. (1973). Vapor–liquid equilibria in mixtures of water, *n*-propanol, and *n*-butanol. *Journal of Chemical and Engineering Data*, *18*, 44–49. https://doi.org/10.1021/je60056a013

Defay, R., Prigogine, I., & Bellemans, A. (1966). *Surface tension and adsorption*. London: Longmans Green & Co.

Djikaev, Y. S., & Ruckenstein, E. (2014). Thermodynamics of water condensation on a primary marine aerosol coated by surfactant organic molecules. *Journal of Physical Chemistry A*, *118*, 9879–9889. https://doi.org/10.1021/jp505578a

Donaldson, D. J., & Vaida, V. (2006). The influence of organic films at the air–aqueous boundary on atmospheric processes. *Chemical Reviews*, *106*, 1445–1461. https://doi.org/10.1021/cr040367c

Eberhart, J. G. (1966). The surface tension of binary liquid mixtures. *Journal of Physical Chemistry*, *70*, 1183–1186. https://doi.org/10.1021/j100876a035

Ellison, G. B., Tuck, A. F., & Vaida, V. (1999). Atmospheric processing of organic aerosols. *Journal of Geophysical Research*, *104*(D9), 11,633–11,641. https://doi.org/10.1029/1999JD900073

Facchini, M. C., Mircea, M., Fuzzi, S., & Charlson, R. J. (1999). Cloud albedo enhancement by surface-active organic solutes in growing droplets. *Nature*, *401*, 257–259. https://doi.org/10.1038/45758

Forestieri, S. D., Staudt, S. M., Kuborn, T. M., Faber, K., Ruehl, C. R., Bertram, T. H., & Cappa, C. D. (2018). Establishing the impact of model surfactants on cloud condensation nuclei activity of sea spray aerosol mimics. *Atmospheric Chemistry and Physics*, *18*, 10,985–11,005. https://doi.org/10.5194/acp-18-10985-2018

Freedman, M. A. (2017). Phase separation in organic aerosol. *Chemical Society Reviews*, *46*, 7694–7705. https://doi.org/10.1039/c6cs00783j

Ghan, S. J., Abdul-Razzak, H., Nenes, A., Ming, Y., Liu, X., Ovchinnikov, M., et al. (2011). Droplet nucleation: Physically-based parameterizations and comparative evaluation. *Journal of Advances in Modeling Earth Systems*, *3*, M10001. https://doi.org/10.1029/2011MS000074

Ghosh, D., Manka, A., Strey, R., Seifert, S., Winans, R. E., & Wyslouzil, B. E. (2008). Using small angle X-ray scattering to measure the homogeneous nucleation rates of *n*-propanol, *n*-butanol, and *n*-pentanol in supersonic nozzle expansions. *Journal of Chemical Physics*, *129*, 124302. https://doi.org/10.1063/1.2978384

Gibbs, J. W. (1878). On the equilibrium of heterogeneous substances (concluded). *Transactions of the Connecticut Academy of Arts and Sciences*, *3*, 343–524.

Giddings, W. P., & Baker, M. B. (1977). Source and effects of monolayers on atmospheric water droplets. *Journal of the Atmospheric Sciences*, *34*, 1957–1964. https://doi.org/10.1175/1520-0469(1977)034<1957

Gill, P. S., Graedel, T. E., & Weschler, C. J. (1983). Organic films on atmospheric aerosol particles, fog droplets, cloud droplets, raindrops, and snowflakes. *Reviews of Geophysics and Space Physics*, *21*, 903–920. https://doi.org/10.1029/RG021i004p00903

Gmehling, J., & Onken, U. (1977). *Vapor–liquid equilibrium data collection, aqueous–organic systems* Chemistry Data Series (Vol. 1). Frankfurt: DECHEMA.

Gorbunov, B., Hamilton, R., Clegg, N., & Toumi, R. (1998). Water nucleation on aerosol particles containing both organic and soluble inorganic substances. *Atmospheric Research*, *47–48*, 271–283. https://doi.org/10.1016/S0169-8095(98)00035-0

Hänel, G. (1976). The properties of atmospheric aerosol particles as functions of the relative humidity at thermodynamic equilibrium with the surrounding moist air. *Advances in Geophysics*, 73–188. https://doi.org/10.1016/S0065-2687(08)60142-9

Hansen, A. M. K., Hong, J., Raatikainen, T., Kristensen, K., Ylisirniö, A., Virtanen, A., et al. (2015). Hygroscopic properties and cloud condensation nuclei activation of limonene-derived organosulfates and their mixtures with ammonium sulfate. *Atmospheric Chemistry and Physics*, *15*, 14,071–14,089. https://doi.org/10.5194/acp-15-14071-2015

Henson, B. F. (2007). An adsorption model of insoluble particle activation: Application to black carbon. *Journal of Geophysical Research*, *112*, D24S16. https://doi.org/10.1029/2007JD008549

Hyvärinen, A.-P., Lihavainen, H., Gaman, A., Vairila, L., Ojala, H., Kulmala, M., & Viisanen, Y. (2006). Surface tensions and densities of oxalic, malonic, succinic, maleic, malic, and cis-pinonic acid. *Journal of Chemical and Engineering Data*, *51*, 255–260. https://doi.org/10.1021/je050366x

Janz, G. J. (1980). Molten salts as reference standards for density, surface tension, viscosity and electrical conductance: KNO_3 and NaCl. *Journal of Physical and Chemical Reference Data*, *9*, 791–829. https://doi.org/10.1063/1.555634

Kodama, M., & Miura, M. (1972). The second CMC of the aqueous solution of sodium dodecyl sulfate. II. Viscosity and density. *Bulletin of the Chemical Society of Japan*, *45*, 2265–2269. https://doi.org/10.1246/bcsj.45.2265

Köhler, H. (1936). The nucleus in and growth of hygroscopic droplets. *Transactions of the Faraday Society*, *32*, 1152–1161. https://doi.org/10.1039/TF9363201152

Krisch, M. J., D'Auria, R., Brown, M. A., Tobias, D. J., Hemminger, J. C., Ammann, M., et al. (2007). The effect of an organic surfactant on the liquid–vapor interface of an electrolyte solution. *Journal of Physical Chemistry C*, *111*, 13,497–13,509. https://doi.org/10.1021/jp073078b

Kristensen, T. B., Prisle, N. L., & Bilde, M. (2014). Cloud droplet activation of mixed model HULIS and NaCl particles: Experimental results and κ-Köhler theory. *Atmospheric Research*, *137*, 167–175. https://doi.org/10.1016/j.atmosres.2013.09.017

Kumar, M. K., & Ghosh, P. (2006). Coalescence of air bubbles in aqueous solutions of ionic surfactants in presence of inorganic salt. *Chemical Engineering Research and Design*, *84*, 703–710. https://doi.org/10.1205/cherd05058

Laaksonen, A. (1993). The composition size dependence of aerosols created by dispersion of surfactant solutions. *Journal of Colloid and Interface Science*, *159*, 517–519. https://doi.org/10.1006/jcis.1993.1358

Laaksonen, A., & Kulmala, M. (1991). An explicit cluster model for binary nuclei in water–alcohol systems. *Journal of Chemical Physics*, *95*, 6745–6748. https://doi.org/10.1063/1.461513

Laaksonen, A., & Malila, J. (2016). An adsorption theory of heterogeneous nucleation of water vapour on nanoparticles. *Atmospheric Chemistry and Physics*, *16*, 135–143. https://doi.org/10.5194/acp-16-135-2016

Langmuir, I. (1917). The constitution and fundamental properties of solids and liquids. II. Liquids. *Journal of the American Chemical Society*, *39*, 1848–1906. https://doi.org/10.1021/ja02254a006

Li, X., Hede, T., Tu, Y., Leck, C., & Ågren, H. (2010). Surface-active cis-pinonic acid in atmospheric droplets: A molecular dynamics study. *Journal of Physical Chemistry Letters*, *1*, 769–773.

Li, Z. X., Lu, J. R., Thomas, R. K., Rennie, A. R., & Penfold, J. (1996). Neutron reflection study of butanol and hexanol adsorbed at the surface of their aqueous solutions. *Journal of the Chemical Society, Faraday Transactions*, *92*, 565–572. https://doi.org/10.1039/FT9969200565

Li, Z., Williams, A. L., & Rood, M. J. (1998). Influence of soluble surfactant properties on the activation of aerosol particles containing inorganic solute. *Journal of the Atmospheric Sciences*, *55*, 1859–1866. https://doi.org/10.1175/1520-0469(1998)055<1859:IOSSPO>2.0.CO;2

Lin, J. J., Malila, J., & Prisle, N. L. (2018). Cloud droplet activation of organic–salt mixtures predicted from two model treatments of the droplet surface. *Environmental Science: Processes and Impacts*, *20*, 1611–1629. https://doi.org/10.1039/C8EM00345A

McFiggans, G., Artaxo, P., Baltensberger, U., Coe, H., Facchini, M. C., Feingold, G., et al. (2006). The effect of physical and chemical properties on warm cloud droplet activation. *Atmospheric Chemistry and Physics*, *6*, 2593–2649. https://doi.org/10.5194/acp-6-2593-2006

Ming, Y., & Russell, L. M. (2001). Predicted hygroscopic growth of sea salt aerosol. *Journal of Geophysical Research*, *106*(D22), 28,259–28,274. https://doi.org/10.1029/2001JD000454

Ming, Y., & Russell, L. M. (2002). Thermodynamic equilibrium of organic–electrolyte mixtures in aerosol particles. *AIChE Journal*, *48*, 1331–1348. https://doi.org/10.1002/aic.690480619

Nozière, B., Baduel, C., & Jaffrezo, J.-L. (2014). The dynamic surface tension of atmospheric aerosol surfactants reveals new aspects of cloud activation. *Nature Communications*, *5*, 3335. https://doi.org/10.1038/ncomms4335

Öhrwall, G., Prisle, N. L., Ottosson, N., Werner, J., Ekholm, V., Walz, M.-M., & Björneholm, O. (2015). Acid–base speciation of carboxylate ions in the surface region of aqueous solutions in the presence of ammonium and aminium ions. *Journal of Physical Chemistry B*, *119*, 4033–4040. https://doi.org/10.1021/jp509945g

Ovadnevaite, J., Zuend, A., Laaksonen, A., Sanchez, K. J., Roberts, G., Ceburnis, D., et al. (2017). Surface tension prevails over solute effect in organic-influenced cloud droplet activation. *Nature*, *546*, 637–641. https://doi.org/10.1038/nature22806

Pajunoja, A., Lambe, A. T., Hakala, J., Rastak, N., Cummings, M. J., Brogan, J. F., et al. (2015). Adsorptive uptake of water by semisolid secondary organic aerosols. *Geophysical Research Letters*, *42*, 3063–3068. https://doi.org/10.1002/2015GL063142

Pegram, L. M., & Record, M. T. (2006). Partitioning of atmospherically relevant ions between bulk water and the water/vapor interface. *Proceedings of the National Academy of Sciences U.S.A.*, *103*, 14,278–14,281. https://doi.org/10.1073/pnas.0606256103

Persson, C. M., Jonsson, A. P., Bergström, M., & Eriksson, J. C. (2003). Testing the Gouy-Chapman theory by means of surface tension measurements for SDS-NaCl-H_2O mixtures. *Journal of Colloid and Interface Science*, *267*, 151–154. https://doi.org/10.1016/S0021-9797(03)00761-6

Petters, M. D., & Kreidenweis, S. M. (2013). Single parameter representation of hygroscopic growth and cloud condensation nucleus activity—Part 3: Including surfactant partitioning. *Atmospheric Chemistry and Physics*, *13*, 1081–1091. https://doi.org/10.5194/acp-13-1081-2013

Petters, S. S., & Petters, M. D. (2016). Surfactant effect on cloud condensation nuclei for two-component internally mixed aerosols. *Journal of Geophysical Research: Atmospheres*, *121*, 1878–1895. https://doi.org/10.1002/2015JD024090

Popovicheva, O. B., Parsiantseva, N. M., Tishkova, V., Shonija, N. K., & Zubareva, N. A. (2008). Quantification of water uptake by soot particles. *Environmental Research Letters*, *3*, 025009. https://doi.org/10.1088/1784-9326/3/025009

Pöschl, U., Rudich, Y., & Ammann, M. (2007). Kinetic model framework for aerosol and cloud surface chemistry and gas–particle interactions—Part 1: General equations, parameters, and terminology. *Atmospheric Chemistry and Physics*, *7*, 5989–6023. https://doi.org/10.5194/acp-7-5989-2007

Prisle, N., Asmi, A., Topping, D., Partanen, A.-I., Romakkaniemi, S., Dal Maso, M. D., et al. (2012). Surfactant effects in global simulation of cloud droplet activation. *Geophysical Research Letters*, *39*, L05802. https://doi.org/10.1029/2011GL050467

Prisle, N. L., Dal Maso, M., & Kokkola, H. (2011). A simple representation of surface active organic aerosol in cloud droplet formation. *Atmospheric Chemistry and Physics*, *11*, 4073–4083. https://doi.org/10.5194/acp-11-4073-2011

Prisle, N. L., Ottosson, N., Öhrwall, G., Söderström, J., Dal Maso, M., & Björneholm, O. (2012). Surface/bulk partitioning and acid/base speciation of aqueous decanoate: Direct observations and atmospheric implications. *Atmospheric Chemistry and Physics*, *12*, 12,227–12,242. https://doi.org/10.5194/acp-12-12227-2012

Prisle, N. L., Raatikainen, T., Laaksonen, A., & Bilde, M. (2010). Surfactants in cloud droplet activation: Mixed organic–inorganic particles. *Atmospheric Chemistry and Physics*, *10*, 5663–5638. https://doi.org/10.5194/acp-10-5663-2010

Prisle, N. L., Raatikainen, T., Sorjamaa, R., Svenningson, B., Laaksonen, A., & Bilde, M. (2008). Surfactant partitioning in cloud droplet activation: A study of C8, C10, C12 and C14 normal fatty acid sodium salts. *Tellus B*, *60*, 416–431. https://doi.org/10.1111/j.1600-0889.2008.00352.x

Raatikainen, T., & Laaksonen, A. (2011). A simplified treatment of surfactant effects on cloud drop activation. *Geoscientific Model Development*, *4*, 107–116. https://doi.org/10.5194/gmd-3-635-2010

Raina, G., Kulkarni, G. U., & Rao, C. N. R. (2001). Surface enrichment in alcohol–water mixtures. *Journal of Physical Chemistry A*, *105*, 10,204–10,207. https://doi.org/10.1021/jp011190i

Richmond, G. L. (2001). Structure and bonding of molecules at aqueous surfaces. *Annual Review of Physical Chemistry*, *52*, 357–389. https://doi.org/10.1146/annurev.physchem.52.1.357

Romakkaniemi, S., Kokkola, H., Smith, J. N., Prisle, N. L., Schwier, A. N., McNeill, V. F., & Laaksonen, A. (2011). Partitioning of semivolatile surface-active compounds between bulk, surface and gas phase. *Geophysical Research Letters*, *38*, L03807. https://doi.org/10.1029/2010GL046147

Rossignol, S., Tinel, L., Bianco, A., Passananti, M., Brigante, M., Donaldson, D. J., & George, C. (2016). Atmospheric photochemistry at a fatty acid-coated air-water interface. *Science*, *353*, 699–702. https://doi.org/10.1126/science.aaf3617

Rothfuss, N. E., Marsh, A., Rovelli, G., Petters, M. D., & Reid, J. P. (2018). Condensation kinetics of water on amorphous aerosol particles. *Journal of Physical Chemistry Letters*, *9*, 3708–3713. https://doi.org/10.1021/acs.jpclett.8b01365

Rowe, A. M., & Chou, J. C. S. (1970). Pressure-volume-temperature-concentration relation of aqueous NaCl solution. *Journal of Chemical and Engineering Data*, *15*, 61–66. https://doi.org/10.1021/je60044a016

Ruehl, C. R., Davies, J. F., & Wilson, K. R. (2016). An interfacial mechanism for cloud droplet formation on organic aerosols. *Science*, *351*, 1447–1450. https://doi.org/10.1126/science.aad4889

Ruehl, C. R., & Wilson, K. R. (2014). Surface organic monolayers control the hygroscopic growth of submicrometer particles at high relative humidity. *Journal of Physical Chemistry A*, *118*, 3952–3966. https://doi.org/10.1021/jp502844g

Rusanov, A. I. (1978). *Phasengleichgewichte und Grenzflächenerschunge*. Berlin: Akademie-Verlag.

Salonen, M., Malila, J., Napari, I., & Laaksonen, A. (2005). Evaluation of surface composition of surface active water–alcohol type mixtures: A comparison of empirical models. *Journal of Physical Chemistry B*, *109*, 3472–3479. https://doi.org/10.1021/jp047610w

Schwier, A. N., Sareen, N., Lathem, T. L., Nenes, A., & McNeill, V. F. (2011). Ozone oxidation of oleic acid surface films decreases aerosols cloud condensation nuclei activity. *Journal of Geophysical Research*, *116*, D16202. https://doi.org/10.1029/2010JD015520

Seidl, W. (2000). Model for a surface film of fatty acids on rain water and aerosol particles. *Atmospheric Environment*, *34*, 4917–4932. https://doi.org/10.1016/S1352-2310(00)00198-9

Shiraiwa, M., Zuend, A., Bertram, A. K., & Seinfeld, J. H. (2013). Gas–particle partitioning of atmospheric aerosols: Interplay of physical state, non-ideal mixing and morphology. *Physical Chemistry Chemical Physics*, *15*, 11,441–11,453. https://doi.org/10.1039/C3CP51595H

Shulman, M. L., Jacobson, M. C., Charlson, R. J., Synovec, R. E., & Young, T. E. (1996). Dissolution behavior and surface tension effects of organic compounds in nucleating cloud droplets. *Geophysical Research Letters*, *23*, 277–280. https://doi.org/10.1029/95GL03810

Sorjamaa, R., & Laaksonen, A. (2006). The influence of surfactant properties on critical supersaturations of cloud condensation nuclei. *Journal of Aerosol Science*, *37*, 1730–1736. https://doi.org/10.1016/j.jaerosci.2006.07.004

Sorjamaa, R., & Laaksonen, A. (2007). The effect of H_2O adsorption on cloud drop activation on insoluble particles: A theoretical framework. *Atmospheric Chemistry and Physics*, *7*, 6175–6180. https://doi.org/10.5194/acp-7-6175-2007

Sorjamaa, R., Svenningson, B., Raatikainen, T., Henning, S., Bilde, M., & Laaksonen, A. (2004). The role of surfactants in Köhler theory reconsidered. *Atmospheric Chemistry and Physics*, *4*, 2107–2117. https://doi.org/10.5194/acp-4-2107-2004

Sprow, F. B., & Prausnitz, J. M. (1966). Surface tensions of simple liquid mixtures. *Transactions of the Faraday Society*, *62*, 1105–1111. https://doi.org/10.1039/TF9666201105

Stewart, D. J., Cai, C., Nayler, J., Preston, T. C., Reid, J. P., Krieger, U. K., et al. (2015). Liquid–liquid phase separation in mixed organic/inorganic single aqueous aerosol droplets. *Journal of Physical Chemistry A*, *119*, 4177–4190. https://doi.org/10.1021/acs.jpca.5b01658

Strey, R., & Schmeling, T. (1983). Surface tension measurements for the *n*-alcohols in temperature range -40° C to +40° C. *Berichte der Bunsengesellschaft für physikalische Chemie*, *87*, 324–327. https://doi.org/10.1002/bbpc.19830870411

Sun, L., Hede, T., Tu, Y., Leck, C., & Ågren, H. (2013). Combined effect of glycine and sea salt on aerosol cloud droplet activation predicted by molecular dynamics simulations. *Journal of Physical Chemistry A*, *117*, 10,746–10,752. https://doi.org/10.1021/jp407538x

Topping, D. (2010). An analytical solution to calculate bulk mole fractions for any number of components in aerosol droplets after considering partitioning to a surface layer. *Geoscientific Model Development*, *3*, 635–642. https://doi.org/10.5194/gmd-3-635-2010

Topping, D. O., McFiggans, G. B., & Coe, H. (2005). A curved multi-component aerosol hygroscopicity framework: Part 2—Including organic compounds. *Atmospheric Chemistry and Physics*, *5*, 1223–1242. https://doi.org/10.5194/acp-5-1223-2005

Topping, D. O., McFiggans, G. B., Kiss, G., Varga, Z., Facchini, M. C., Decesari, S., & Mircea, M. (2007). Surface tensions of multicomponent mixed inorganic/organic aqueous systems of atmospheric significance: Measurements, model predictions and importance for cloud activation predictions. *Atmospheric Chemistry and Physics*, *7*, 2371–2398. https://doi.org/10.5194/acp-7-2371-2007

Toribio, A. N., Prisle, N. L., & Wexler, A. S. (2018). Statistical mechanics of multilayer sorption: Surface concentration modeling and XPS measurement. *Journal of Physical Chemistry Letters*, *9*, 1461–1464. https://doi.org/10.1021/acs.jpclett.8b00332

Vanhanen, J., Hyvärinen, A.-P., Anttila, T., Raatikainen, T., Viisanen, Y., & Lihavainen, H. (2008). Ternary solution of sodium chloride, succinic acid and water; surface tension and its influence on cloud droplet activation. *Atmospheric Chemistry and Physics*, *8*, 4595–4604. https://doi.org/10.5194/acp-8-4595-2008

Vehkamäki, H. (2006). *Classical nucleation theory in multicomponent systems*. Berlin: Springer.

von Szyszkowski, B. (1908). Experimentelle Studien über kapillare Eigenschaften der wässrigen Lösungen von Fettsäuren. *Zeitschrift für physikalische Chemie*, *64*, 385–414. https://doi.org/10.1515/zpch-1908-6425

Walz, M.-M., Caleman, C., Werner, J., Ekholm, V., Lundberg, D., Prisle, N. L., et al. (2015). Surface behavior of amphiphiles in aqueous solution: A comparison between different pentanol isomers. *Physical Chemistry Chemical Physics*, *17*, 14,063–14,044. https://doi.org/10.1039/c5cp01870f

Walz, M.-M., Werner, J., Ekholm, V., Prisle, N. L., Öhrwall, G., & Björneholm, O. (2016). Alcohols at the aqueous surface: Chain length and isomer effects. *Physical Chemistry Chemical Physics*, *18*, 6648–6656. https://doi.org/10.1039/c5cp06463e

Werner, J., Dalirian, M., Walz, M.-M., Ekholm, V., Wideqvist, U., Lowe, S. J., et al. (2016). Surface partitioning in organic–inorganic mixtures contributes to the size-dependence of of the phase-state of atmospheric nanoparticles. *Environmental Science and Technology*, *50*, 7434–7442. https://doi.org/10.1021/acs.est.6b00789

Werner, J., Julin, J., Dalirian, M., Prisle, N. L., Öhrwall, G., Persson, I., et al. (2014). Succinic acid in aqueous solution: Connecting microscopic surface composition and macroscopic surface tension. *Physical Chemistry Chemical Physics*, *16*, 21,486–21,495. https://doi.org/10.1039/c4cp02776k

Wexler, A. S., & Dutcher, C. S. (2013). Statistical mechanics of multilayer sorption: Surface tension. *Journal of Physical Chemistry Letters*, *4*, 1723–1726. https://doi.org/10.1021/jz400725p

Wölk, J., & Strey, R. (2001). Homogeneous nucleation of H_2O and D_2O in comparison: The isotope effect. *Journal of Physical Chemistry B*, *105*, 11,683–11,701. https://doi.org/10.1021/jp0115805

Wyslouzil, B. E., Wilemski, G., Strey, R., Heath, C. H., & Dieregsweiler, U. (2006). Experimental evidence for internal structure in aqueous–organic nanodroplets. *Physical Chemistry Chemical Physics*, *8*, 54–57. https://doi.org/10.1039/b514824c

Zuend, A., & Seinfeld, J. H. (2013). A practical method for the calculation of liquid–liquid equilibria in multicomponent organic–water–electrolyte systems using physicochemical constraints. *Fluid Phase Equilibria*, *337*, 201–213. https://doi.org/10.1016/j.fluid.2012.09.034